Common Spatial Pattern for Human Identification Based on Finger Vein Images in Radon space

Akram Gholami✉, Hamid Hassanpour

Department of Computer Engineering & IT, Shahrood University of Technology, Shahrood, Iran

a_gholami677@yahoo.com; h_hassanpour@yahoo.com

Abstract

Finger vein is one of the most fitting biometric for identifying individuals. In this paper a new method for finger vein recognition is proposed. First the veins are extracted from finger vein images by using entropy based thresholding. In finger vein images the veins are appeared as dark lines. The method extracts veins as well, but the images are noisy, that means in addition to the veins they have some short and long lines. Then radon transformation are applied to segmented images. The Radon transform is not sensitive to the noise in the images due to its integral nature, so in comparison with other methods is more resistant to noise. For extracting dominant features from finger vein images, common spatial patterns (CSP) is applied to the blocks of radon transformation. Finally the data classified by using nearest neighbor (1-NN) and multilayer perceptron (MLP) neural network. The research was performed on the Peking University finger vein dataset. Experimental results show that 1-NN using CSP, with detecting rate 99.6753%, against MLP is most appropriate for finger vein recognition.

Keywords: Finger Vein Recognition, Local Entropy Thresholding, Radon Transform, Common Spatial Patterns(CSP), 1-Nearest Neighbour(1-NN) Classifier, Multilayer Perceptron (MLP) Neural Network

1. Introduction

Biometric identifiers are unique to individual. Several types of biometric identification system exist , such as fingerprint, face, voice, iris, hand vein and etc. These Biometric techniques mentioned in certain circumstances have some limitations [1]. But finger vein is a suitable biometric. Every finger has a unique pattern of veins that can be used to identify individuals. In addition, vein recognition technology has the following features [1,3]. 1.Noncontact, 2.Identification of living body, 3.High security and 4.Small device size. These favorable properties caused the vein recognition to be a very reliable method of identification.

Finger vein recognition process includes four steps:1.Image acquisition 2.Image processing 3.Feature extraction and 4. Matching [1,2]. In the first step, infrared light is emitted to skin. By this work the situation of veins that are located under the skin is achieved. Preprocessing step contains image enhancement, noise removal and normalization [1,2]. Segmentation is a vital step and some methods are used for this purpose [1,2]. Miura et al. [4] extract finger vein pattern by using repeated line tracking algorithm, which starts from a different position. Minutiea features are extracted from

the vein patterns in [5]. Minutiea points consist of ending and bifurcation points, which are used to display geometrical shape of patterns. In [6] authors have proposed mean curvature method that by considering vein image as a geometric shape, finds valley-like structures with negative mean curvatures. finger vein patterns in [7] are extracted by combining two segmentation methods, including morphological operators and maximum curvature points of the profile of the image. In [8] a wide line detector is used for extracting features, that in addition to obtain detailed information for veins, information about extracted features from low-quality images is increased. In [9] authors use a 2-D Gabor filter to filter the original finger vein image, then the phase and direction texture features are extracted and coded. Then modified Hamming distance is used for measuring the similarity.

In this paper, we used local entropy thresholding for image segmentation. This method has a good performance in vein extraction, but the segmented images are noisy. This means that in addition to the veins that appear as dark lines, number of short and long lines are in the segmented images. Then we applied Radon Transform on the segmented images. Radon transform due to the integral nature resistance to noise. This transformation is used for images that have important lines. It transforms images which include lines into a space and contain lines characteristics. With this transformation, we don't need to extract lines from images accurately, hence recognition accuracy and speed are increased. For extracting features of finger vein images, common spatial pattern (CSP) is applied on the blocks of radon transformation. CSP bacically are used to extract features from EEG signals, but because of different color components of the color image (radon image) are similar to different channels in EEG signals, in this paper we used CSP to extract fearures from RGB images. Finally we used multilayer perceptron (MLP) neural network and the nearest neighbor (1-NN) method to classify data.

The rest of this paper is organized as follows: Segmentation will be introduced in Section 2. Radon Transformation will be explained in section 3. Feature extraction by CSP is explained in section 4. The proposed method will be described in Section 5. Experimental results are demonstrated in Section 6 to verify the validity of the proposed method. Finally, Section 7 concludes this paper.

2. Segmentation

After noise reduction and contrast improving, segmentation leads to separate the vein patterns from background. In fact, the vein patterns are located and separated from the rest of the image. Segmentation is an important step in the recognition process and there are some methods for this purpose. In this study we used local entropy thresholding for image segmentation.

2. 1. Local entropy thresholding

Thresholding became an effective tool for image segmentation. There are several methods for thresholding, one of them is local entropy thresholding. The entropy based thresholding that use gray level co-occurrence matrix is employed[12]. Due intensities of an image pixel are not independent of each other, it takes into account the spatial distribution of gray levels [12]. Chiefly we implement a local entropy thresholding technique, described in [14]. The co-occurrence matrix of the image F is an P*Q dimensional matrix(denoted by $T = [t_{ij}]$P*Q) [10]. Elements of co-occurrence matrix

32

are specified by the numbers of transitions between all pairs of grey levels in a specified way [12]. Various definitions of co-occurrence matrix depending upon the ways in which the gray level i follows gray level j, are possible [12]. A widly used co-occurrence matrix is an asymmetric matrix which only considers the gray level transitions between two adjacent pixels [13]. By considering horizontally right and vertically lower transitions the co-occurrence matrix is presented as:

$$t_{ij} = \sum_{i=1}^{P}\sum_{k=1}^{Q}\delta \tag{1}$$

$$\delta = 1 \quad \text{if} \begin{cases} f(l,k)=i \text{ and } f(l,k+1)=j \\ \qquad \text{or} \\ f(l,k)=i \text{ and } f(l+1,k)=j \end{cases} \tag{2}$$

$$\delta = 0 \quad \text{otherwise}$$

A desired transition probability from gray level i to gray level j (denoted by p_{ij}) can be defined as:

$$p_{ij} = \frac{t_{ij}}{\sum_i\sum_j t_{ij}} \tag{3}$$

If s, $0 \leq s \leq L\text{-}1$, is a threshold then s can partition the co-occurrence matrix into 4 quadrants, namely A, B, C, and D [12] (Figure 1).
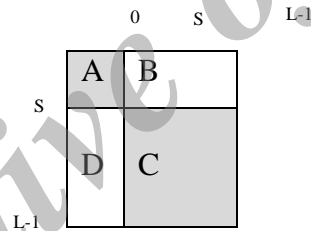

Figure 1: Quadrants of co-occurrence matrix [14].

By considering only quadrants A and C local entropic threshold is given by [12].

$$P_A = \sum_{i=0}^{S}\sum_{j=0}^{S} p_{ij} \tag{4}$$

$$P_C = \sum_{i=s+1}^{L-1}\sum_{j=s+1}^{L-1} p_{ij} \tag{5}$$

The normalized probabilities of the background class and object class are presented as [12]:

$$P_{ij}^{A} = \frac{p_{ij}}{P_A} = \frac{t_{ij}\Big/ (\sum_{i=0}^{L-1} t_{ij})}{\sum_{i=0}^{8}\sum_{j=0}^{8} t_{ij} \Big/ \sum_{i=0}^{L-1}\sum_{j=0}^{L-1} t_{ij}} = \frac{t_{ij}}{\sum_{i=0}^{8}\sum_{j=0}^{8} t_{ij}}, \qquad \text{for } 0 \leq i \leq s, \, 0 \leq j \leq s \tag{6}$$

$$P_{ij}^{c} = \frac{p_{ij}}{P_C} = \frac{t_{ij}}{\sum\limits_{i=s+1}^{L-1}\sum\limits_{j=s+1}^{L-1} t_{ij}}, \text{for } s+1 \le i \le L-1, \, s+1 \le j \le L-1 \tag{7}$$

The second-order entropy of the object given by [12]:

$$H_A^{(2)}(S) = -\frac{1}{2}\sum\limits_{i=0}^{S}\sum\limits_{j=0}^{S} P_{ij}^{A} \log_2 P_{ij}^{A} \tag{8}$$

Similarly, the second-order entropy of the background can be defined as[12]:

$$H_C^{(2)}(S) = -\frac{1}{2}\sum\limits_{i=s+1}^{L-1}\sum\limits_{j=s+1}^{L-1} P_{ij}^{c} \log_2 P_{ij}^{c} \tag{9}$$

By summing up the local entropies of the object and the background, the second-order local entropy can be obtained by [13]:

$$H_T^{(2)}(S) = H_A^{(2)}(S) + H_C^{(2)}(S) \tag{10}$$

The gray level corresponding to the maximum of $H_T^{(2)}(s)$ gives the optimal threshold for object-background classification [12] and can be written as:

$$T_E = \arg\left[\max_{T=0...L-1} H_T^{(2)}(S)\right] \tag{11}$$

Figure2 shows two finger vein image that finger vein patterns are extracted by using local entropy thresholding. As we can see the veins are extracted as well, but the segmented images are some noisy. That means in addition to the veins that appeared as dark lines, they have some short and long lines. Radon transform due to the integral nature is not sensitive to noise ratio and high resistance against noise, so we have used this transform. We applied radon transform to the segmented images.
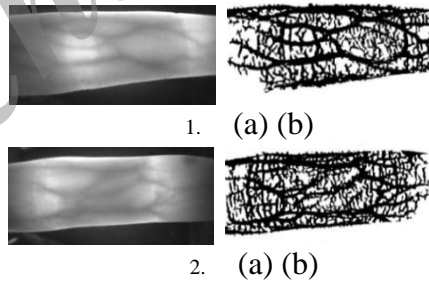

1. (a) (b)

2. (a) (b)

Figure 2: Segmentation, 1(a) , 2(a) finger vein images and 1(b) , 2(b) local entropy thresholding

3. Radon transformation

The radon transform is a mathematical technique [15]. Radon transform is able to transform two dimensional images with lines into a domain that contains parameters of these lines. That means each line in the image will give a peak positioned at the corresponding line parameters [16,17]. The Radon transform by integrating the intensity of the image in all possible orientations is very useful in detecting and locating lines in the image [18]. A 2-D discrete Radon transform called Hough transform [15]. The radon transform can be presented as:

34

$$R(r,\theta) = \int\limits_{-\infty}^{\infty} \int\limits_{-\infty}^{\infty} f(x,y)\delta(x\cos\theta + y\sin\theta - r)dxdy \tag{12}$$

Where δ is the dirac delta function, θ is the orientation and r is perpendicular distance of a line from [16,19]. Rotation, , scaling, linearity skewing are the properties of radon transform [16]. These characteristics simultaneously with their ability to detect lines in an environment with high noise levels, are main motivation for its selection as a tool for image analysis. Figure 3 shows the result of applying the radon transform on two different images corresponding to two different persons.
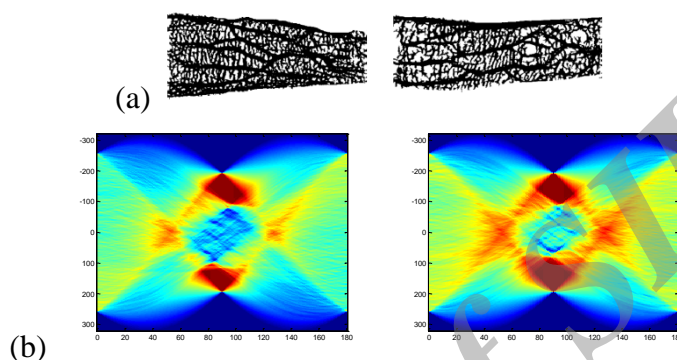

Figure 3: a) finger vein image of two subjects and Radon transformation of them with having θ=0-180 and the same r per each θ

4. Feature extraction

One of the most successful methods for identifying brain patterns, using common spatial patterns (CSP) by Mueller - Grkyng is planned [20]. A useful method for feature extraction of EEG signals is CSP. To record EEG signals from the people's brain several electrodes are placed on the head of people and the final signal is obtained by combining signals from all the electrodes. CSP use different properties of each of these channels and extract appropriate feature from combined signal. Similar to EEG signals the images that are taken to radon transform have three main components R, G and B. So we can use common spatial patterns (CSP) for extract features from this color images. First, the images are divided into equal sized windows. Then the CSP feature extraction method applied on each window, and the feature vectors are extracted from each window. Then we put the feature vectors of all windows together to form the final feature vector.

4. 1. Feature extraction by CSP

First CSP was designed with only two classes of brain patterns recorded by EEG [21]. J.Muller-Gerking proposed multi class extension of CSP, which is based on pairwise classification. As follow, we present multi CSP algorithm.

4. 1.1. The method

CSP without loss of generality can be expanded into several classes. We used this method to classify data in 154 classes. First we change each image into a vector with one row. Consider several subjects that are shown as matrixes Xi, which i represent the class number. Each class size is N × K, where K is number of samples in image matrix

and N is the number of color components that is three. Auto-covariance matrixes for each subject are computed as:

$$R^{(i)} = \sum_{k=1}^{K}(x_k^{(i)} - \frac{1}{k}\sum_{k=1}^{K} x_k^{(i)}) \tag{13}$$

Where $x_k^{(i)}$ is a N-dimensional vector at time k. the index of classes is shown by i that is changed from 1 to 154. t is transpose operator. Normalized covariance matrix are given by:

$$R_i = \frac{1}{l}\sum_{i=1}^{l}\frac{R^{(i)}R'^{(i)}}{trace(R^{(i)}R'^{(i)})} \tag{14}$$

Where normalized covariance matrix is shown by R, and l indicates the numbers of images per subject. Trace(x) is sum of the diagonal elements of x. The composite covariance matrix is computed as follow:

$$R = \sum_{i=1}^{n} R_i \tag{15}$$

That n is number of subjects. Then eigenvalues and eigenvectors should be extracted from matrix R:

$$R = U_0 \Lambda U_0^T \tag{16}$$

Eigenvalue and eigenvector matrix of R are Λ and U0 respectively. The whitening matrix can be defined as:

$$W = \Lambda^{-\frac{1}{2}} U_0^t \tag{17}$$

For extracting common spatial patterns of condition we have:

$$R'_a = \sum_{i \neq a} R_i \tag{18}$$

Then evaluate the transformed covariance matrixes Sa and Sa' respectively, for each class a:

$$S_a = WR_a W^T, \quad S'_a = WR'_a W^T \tag{19}$$

It is evident that sum of corresponding eigenvalues of these matrixes will be one and Sa and S'a share common eigenvectors. So Sa and S'a can be decomposition as:

$$S_a = U\Lambda_a U^T \tag{20}$$

$$S'_a = U\Lambda'_a U^T \tag{21}$$

And following clause is true:

$$\Lambda_a + \Lambda'_a = I \tag{22}$$

Sort the eigenvectors U in respect of the eigenvalues Λa, in descending order (Or in ascending order in respect of Λa'), then the projection matrix is given by:

$$SF_a = UW \tag{23}$$

36

Spatial filter of a condition is SF. class "a" will be yield the maximum variance and class " a' " will be yield the minimum variance, by projecting class "a" and " a' " onto the first Eigenvector U1. Against we will have reverse results, by projecting them into the last Eigenvector U1. i.e. class "a" will be yield minimum variance.

So, we get the mapping of each finger vein image of subject "a" as follow:

$$Z_a = SF_a X_a \qquad (24)$$

By choosing a few Eigenvectors, Um=(U1,…Um,UN-m+1,…,UN), where m is low(m<<N), the projection matrix is defined as:

$$SF_a^s = U_m W \qquad (25)$$

The final projection matrix is given by:

$$Z_a^s = SF_a^s X_a \qquad (26)$$

After calculating Z, for i=1,…,154, suitable features should be extracted from Z. So in last step, calculate the logarithm transformed, normalized variance of Z:

$$f_i^{\,k} = \log\left(\frac{\mathrm{var}(Z_{pi}^{\,k})}{\sum_{p=1}^{2m} \mathrm{var}(Z_p)}\right) \qquad (27)$$

Rows of f_k^i are extracted features related to subject ith. The number of extracted features is equal to the number of selected eigenvectors (m).

5. The proposed method

In this paper a new method of finger vein recognition was proposed, in which the local entropy thresholding is used for extracting finger veins. Also CSP have been used to extract features from finger vein images. Block diagram of the proposed method is shown in Figure 4.
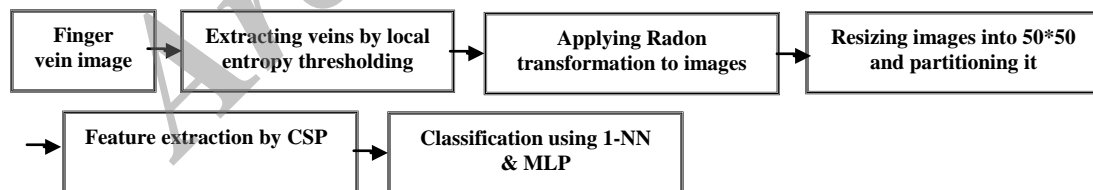

Figure 4: The block diagram of proposed method

Segmentation is an important step in the recognition process. In this study we used local entropy thresholding for this purpose. With this method the veins are extracted as well, but a number of short and long lines that do not belong to veins also extracted and the resulting images are noisy. Radon transform does not require to extract lines exactly and thus increases the accuracy and speed of detection, thus we use this transformation to convert images into Radon space. To extract features from radon images, the images will be resized into the image with size 50 * 50. Radon images are color images that

37

have three color components. Then Radon image with size 3*50 * 50 (where 3 is the number of color components) are converted into 3*2500 vectors. Now by having a vector 3*2500 is representative of each radon image, we can extract features. To extract features from the vector, the components of R and G and B are separated from it. Because the dimension of vectors is too big for CSP, to extract features with CSP, these Vectors are divided into 20 equal-sized windows. Thus, the windows dimensions are 125 (2500/20). Then by applying CSP on each window individually, suitable features are extracted from each window. Then the feature vectors extracted from these windows put together and make the final feature vector. Finally, we use a MLP neural network and the nearest neighbor (1-NN) method to classify the data, and compare their performance with each other.

6. Experimental results

6. 1. Dataset

The experiments have been performed on the PKU(V4) Finger Vein Dataset, which was collected by Peking University [22]. The number of subjects was 200 and finger vein images were obtained from eight fingers of each subject. 46 files are appended a suffix of ignore, which indicates that this sample is not in good quality, marked by human examinant. Then we used images of only 154 subject. 75% of data were used for training system and 25% of it used for testing it. Therefore, the database contains 1232 finger vein images made up of 512×384 pixels. Some examples of finger vein images are shown in Figure 5.
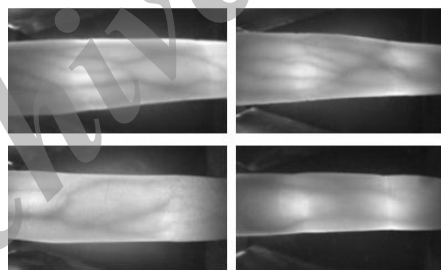

Figure 5: Some example of finger vein images

We tested our proposed method for each classifier on a different number of classes such as: 10, 50, 100 and 154 classes. To evaluate the proposed method we used True Positive measure, that is obtained by dividing the number of corrected classified data on the total number of data.

6. 2. MLP classifier

As the matching alghorithm we used a three-layer MLP neural network. For this network, we consider the number of nodes in the middle of layer seven. The number of nodes in the output layer for the 154 class is eight, in order to the 154 class can be encoded in binary form. Number of nodes in the output layer for 10, 50 and 100 classes respectively are 4,6 and 7. After extracting appropriate features and making the final

feature vector, we take it as on input to the neural network. The number of nodes in the input layer is equal to the length of the feature vector. For MLP classifier by assuming that the network error is MSE, the success rate of the network is obtained from ((1-MSE)*100%).

6. 3. 1-NN classifier

As another method of classification, we used 1-NN classifier. In this method to measure the distance from the test data of training data we used the Manhattan distance.

6. 4. A comparision between MLP and 1-NN classifiers

In this section, a comparison between MLP and 1-NN classifiers in terms of classification accuracy and time spent is done. About the classification accuracy it is shown that the 1-NN method can do Better and have more accurate classification than MLP. The comparison between the classification accuracy of two classifiers for CSP feature has been shown in Figure 6.

As you can see in the Figure 6, MLP only for 10 classes is good and obtained the success rate of 95.6612%. However, by increasing the number of classes a success rate using MLP (CSPMLP method) is strongly discouraged. While by using 1-NN as classifier (CSP1-NN method) good performance has achieved and the success rate for different number of classes is high. So that for the 50 and 100 Classes the success rate is 100% and for the 154 class the success rate of 99.6753% is obtained. Also a comparison between the time spent of two classifiers is done in Figure 7. As we can see the performance of two classifiers in terms of time consumption are close together. But the success rate by using these two classifiers are very different.
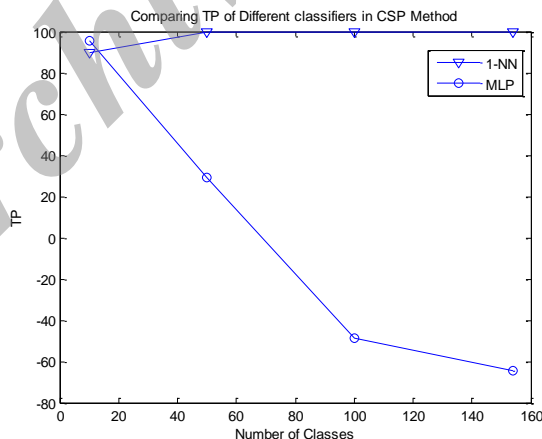

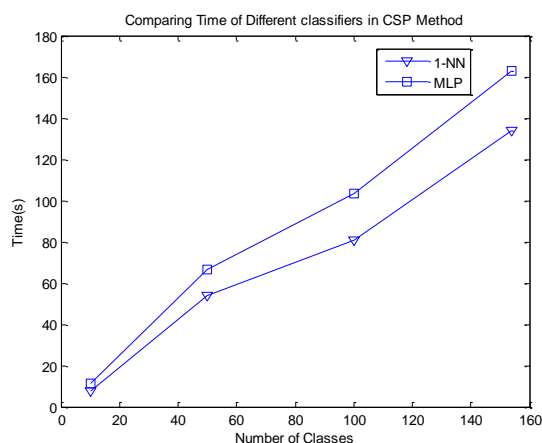*Figure 6: Comparison of classifier performance in terms of success rate*

Figure 7: Comparison of classifier performance in terms of time consumption

Overall, the results (Table 1) show that the proposed method CSP1-NN in comparison with CSPMLP and other methods in the literature, in terms of high identification rate is very good. This method can identify individuals via finger vein images with a high success rate (99.6753%) in a short time (162.67491 seconds, about 2 minutes).

Table 1. Comparison of classifier performance in CSP method.

Number of classes	CSP1-NN method		CSPMLP method	
	Success Rate(TP)(%)	Time(s)	Network Performance	Time(s)
10	90	7.66	95.6612	11.09
50	100	53.85	29.2712	66.52
100	100	80.83	-48.5461	103.15
154	99.6753	134.13	-64.2792	162.67

7. Conclusion

 In this paper, we proposed a new method for finger vein recognition. First we extracted Vein patterns by using local entropy thresholding. The method extracts veins as well, but the segmented images are noisy. The Radon transform due to the integral nature is more resistant to noise, therefore we applied this transformation on the segmented images. Then we used CSP to extract suitable features from radon images. Radon images are color images that contain three components R, G and B. Because colored components in RGB images are similar to several channels in EEG, CSP has been used to extract features form RGB images. In the proposed method radon images are resized into 50*50 images. Then this matrix 3*50*50 convert into one vector with size 3*2500. Due to the high dimension of these vectors for CSP, we divide it into 20 equal-sized windows. Then by applying CSP on each of these windows separately, we extract the feature vector of each window. Then the feature vectors of all windows were putting together to form the final feature vector. Finally the data were classified using 1-NN and MLP classifier. Experimental results show that the proposed method CSP1-NN (using 1-NN as classifying) has good performance in recognizing individuals based on the finger vein images and in a short time achieves a success rate of 99.6753%.

40

Reference

[1] X.J. Meng, G.P. Yang, Y.L. Yin, R.Y. Xiao, "Finger vein recognition based on local directional code", Sensors, (2012), 12, 14937–14952.

[2] G.P. Yang, X.M. Xi, Y.L.Yin, "Finger vein recognition based on (2D)2PCA and metric learning", J. Biomed. Biotechnol, (2012), 1–9.

[3] G.P. Yang, X.M. Xi , Y.L.Yin, "Finger vein recognition based on a personalized best bit map",Sensors,(2012), 12, 1738–1757.

[4] N. Miura , A. Nagasaka , T. Miyatake,"feature extraction of finger-vein patterns based on repeated line tracking and its application to personal identification", Mach. Vis. Appl, Vol. 15, (2004), 194–203.

[5] C.B. Yu , H.F. Qin, , L. Zhang, , Y.Z. Cui ,"Finger-vein image recognition combining modified hausdorff distance with minutiae feature matching", J. Biomed. Sci. Eng, Vol. 2, (2009), 261–272.

[6] W. Song , T. Kim , H.C. Kim , J.H. Choi , H.J. Kong , S.R. Lee ," A finger-vein verification system using mean curvature", Patt.Recogn.Lett, Vol. 32, (2011), 1541–1547.

[7] N. Miura ,A. Nagasaka, T. Miyatake," Extraction of Finger-Vein Patterns Using Maximum Curvature Points in Image Profiles", In Proceedings of the 9th IAPR Conference on Machine Vision Applications (MVA), Tsukuba, Japan, 16–18 May (2005), 347–350.

[8] B.N. Huang , Y.G. Dai, R.F. Li ," Finger-vein authentication based on wide line detector and pattern normalization", In Proceedings of the 20th International Conference on Pattern Recognition, Istanbul, Turkey, 23–26 August (2010), 1269–1272.

[9] K.J. Wang , J.Y. Liu , P. Popoola Oluwatoyin, W.X. Feng," Finger vein identification based on 2-D gabor filter", In Proceedings of the 2nd International Conference on Industrial Mechatronics and Automation, Wuhan, China, 30–31 May (2010), 10–13.

[10] "Adaptive Thresholding", http://homepages.inf.ed.ac.uk/rbf/HIPR2/adpthrsh.htm, last visited on 10/07/2013

[11] F. Shafait, D. Keysers and T. Breuel, "Efficient implementation of local adaptive thresholding techniques using integral images", Proc. SPIE. [Online]. Available: http://www.dfki.uni-kl.de/_shafait/papers/ Shafait-eficient-binarization-SPIE08.pdf, (2008).

[12] T. Chanwimaluang, and G. Fan, "An efficient blood vessel detection algorithm for retinal images using local entropy thresholding", Proceedings of IEEE International Symposium on Circuits and Systems, Bangkok, Thailand, Vol. 5, (2003), 21-24.

[13] C.I. Chang, K. Chen, J. Wang, M.L.G. Althouse, "A relative entropy-based approach to image thresholding", Pattern Recognit, Vol. 27, (9), (1994), 1275-1289.

[14] N.R. Pal, and S.K. Pal, "Entropic thresholding", Signal processing, Vol. 16, (1989), 97.108.

[15] A. Gavlasov´a, and A. Proch´azka," Simulink Modelling of Radon and Wavelet Transforms for Image Feature Extraction", In International Conference Technical Computing Prague, (2005).

[16] A. Asad, S.A.M. Gilani, U. Shafique, "Affine Invariant Feature Extraction Using a Combination of Radon and Wavelet Transforms", T. Sobh (ed.), Innovations and Advanced Techniques in Computer and Information Sciences and Engineering, 93–97.

[17] X. Jia, J.J. Cui, D.Y. Xue, F. Pan," An Adaptive Dorsal Hand Vein Recognition Algorithm Based on Optimized HMM", Journal of Computational Information Systems, (2012), 313 – 322.

[18] A. Kumar, Y.B. Zhou, "Human identification using finger images", IEEE Trans. Image Process., Vol. 21, (2011),2228–2244.

[19] "Radon Transform", http://homepages.inf.ed.ac.uk/rbf/CVonline/LOCAL_COPIES/AV0405/HAYDEN/Slice_Reconstruction.html, last visited on 01/09/2014.

[20] J. Muller-Gerking, G. Pfurtscheller, and H. Flyvbjerg, "Designing optimal spatial filters for single-trial EEG classification in a movement task" Clin. Neurophysiol, Vol. 110 (5), (1999), 787–798.

[21] E. Niedermeyer, F.H.L.D. Silva, "Electroencephalography: basic principles, clinical applications, and related fields", Lippincott Williams & Wilkins, (2005).

[22] PKU Finger Vein Database (V4) from Peking University. Available online: http://rate.pku.edu.cn/